

Review Article



Recent Advances in Cardiac Magnetic Resonance Imaging

Sang-Eun Lee, MD, PhD^{1,2,3}, Christopher Nguyen, PhD^{3,4,5}, Yibin Xie , PhD³, Zixin Deng, PhD³, Zhengwei Zhou, PhD³, Debiao Li, PhD³, and Hyuk-Jae Chang , MD, PhD^{1,2}

¹Division of Cardiology, Severance Cardiovascular Hospital, Yonsei University College of Medicine, Yonsei University Health System, Seoul, Korea

²Integrative Cardiovascular Imaging Center, Yonsei University Health System, Seoul, Korea

³Biomedical Imaging Research Institute, Cedars-Sinai Medical Center, Los Angeles, CA, USA

⁴Cardiovascular Research Center, Massachusetts General Hospital, Charlestown, MA, USA

⁵Harvard Medical School, Boston, MA, USA



Received: Jul 25, 2018

Revised: Sep 25, 2018

Accepted: Oct 23, 2018

Correspondence to

Hyuk-Jae Chang, MD, PhD

Division of Cardiology, Severance Cardiovascular Hospital, Yonsei-Cedars-Sinai Integrative Cardiovascular Imaging Research Center, Yonsei University College of Medicine, Yonsei University Health System, 50-1, Yonsei-ro, Seodaemun-gu, Seoul 03722, Korea.
E-mail: hjchang@yuhs.ac

Copyright © 2019. The Korean Society of Cardiology

This is an Open Access article distributed under the terms of the Creative Commons Attribution Non-Commercial License (<https://creativecommons.org/licenses/by-nc/4.0>) which permits unrestricted noncommercial use, distribution, and reproduction in any medium, provided the original work is properly cited.

ORCID iDs

Yibin Xie 

<https://orcid.org/0000-0002-0333-567X>

Hyuk-Jae Chang 

<https://orcid.org/0000-0002-6139-7545>

Funding

This study was supported by Leading Foreign Research Institute Recruitment Program through the National Research Foundation of Korea funded by the Ministry of Science, ICT & Future Planning (grant No. 2012027176).

ABSTRACT

Cardiac magnetic resonance (CMR) imaging provides accurate anatomic information and advanced soft contrast, making it the reference standard for assessing cardiac volumes and systolic function. In this review, we summarize the recent advances in CMR sequences. New technical development has widened the use of CMR imaging beyond the simple characterization of myocardial scars and assessment of contractility. These novel CMR sequences offer comprehensive assessments of coronary plaque characterization, myocardial fiber orientation, and even metabolic activity, and they can be readily applied in clinical settings. CMR imaging is able to provide new insights into understanding the pathophysiologic process of underlying cardiac disease, and it can help physicians choose the best treatment strategies. Although several limitations, including the high cost and time-consuming process, have limited the widespread clinical use of CMR imaging so far, recent advances in software and hardware technologies have made the future more promising.

Keywords: Cardiology; Magnetic resonance imaging; Cardiac magnetic resonance

INTRODUCTION

Cardiac magnetic resonance (CMR) imaging provides accurate anatomic information along with advanced soft contrast, which enables superior discrimination of lesions compared to other imaging modalities. Currently, CMR imaging is considered the reference standard for quantification of the cardiac chamber size and systolic function of the heart.¹⁾ Further, tissue characterization techniques including late gadolinium enhancement (LGE), T1 mapping, T2 mapping, and T2-star mapping provide insight into the pathophysiological changes of the myocardium.²⁾³⁾

The drawbacks for the clinical application of CMR imaging have been the long acquisition time, relatively low spatial resolution, and high costs. However, new technical advances in hardware and software components accelerated the image acquisition time, and the introduction of 3T magnetic resonance imaging (MRI) has further improved the spatial resolution and diagnostic accuracy of CMR imaging in the assessment of the myocardium

Conflict of Interest

The authors have no financial conflicts of interest.

Author Contributions

Conceptualization: Chang HJ, Lee SE;
Supervision: Chang HJ, Li D; Writing - original draft: Lee SE; Writing - review & editing: Chang HJ, Lee SE, Nguyen C, Xie Y, Deng Z, Zhou Z, Li D.

and coronary arteries.^{14,15} Consequently, CMR imaging has become one of the routine clinical imaging investigations used for assessing patients with various cardiac diseases.

In this review, we summarize the recent advances in CMR imaging techniques that can readily be applied in clinical practice.

IMAGING AND CHARACTERIZATION OF THE MYOCARDIUM

T1 and T2 mapping

CMR imaging is optimized for characterization of the myocardium through its excellent soft-tissue contrast and various different imaging parameters, and it can provide insight into disease etiologies and the extent and stage of the diseases.^{6,7} Recently, more sophisticated CMR imaging techniques that can provide myocardial tissue characterization beyond the presence of myocardial fibrosis have been introduced.⁸ Native T1 mapping techniques and extracellular volume (ECV) fraction quantification can go beyond LGE imaging and identify more diffuse interstitial fibrosis.^{9,10}

Native T1 value is a composite signal of myocytes and ECV, and is influenced by the field strength, with higher values at 3T than at 1.5T.¹¹ The native T1 mapping does not require gadolinium-based contrast agents and hence is feasible in patients with renal impairment.¹² The native (non-contrast) T1 mapping can detect pathophysiological process including diffuse interstitial fibrosis, myocardial edema, protein deposition, and other T1-altering substances including iron and lipid.¹³ In conditions that causes myocardial edema (e.g. acute myocardial infarction) or an increase of interstitial space (e.g. interstitial fibrosis caused by infarction or cardiomyopathies), the native T1 value increases. In case of lipid (e.g. Anderson-Fabry disease) or iron overload, the native T1 value decreases. Therefore, changes in myocardial T1 reflects various cardiac and systemic conditions.¹²

ECV expansion is a main feature of heart failure, and ECV is a marker of myocardial remodeling.¹⁴ For the calculation of the ECV fraction, contrast-enhanced T1 mapping is used.¹² Gadolinium-based contrast agents are distributed throughout the interstitial space and shorten T1 relaxation times proportional to the local concentration of gadolinium. Therefore, myocardial segments with fibrosis and scar exhibit shorter T1 relaxation times after the contrast administration. Calculation of the ECV requires measurement of myocardial and blood T1 before and after the contrast enhancement. In healthy individuals, normal ECV values of 25.3±3.5% in 1.5T have been reported.¹⁵ An increase in ECV is mostly caused by excessive collagen deposition and is thus represents myocardial fibrosis, and ECV reduces in the presence of thrombus or fat/lipomatous metaplasia.

Both native T1 mapping and ECV can help the differential diagnosis of patients with chest pain, and also can provide information for the distinction of acute from chronic conditions.⁹ Native T1 values of chronic myocardial infarction is lower and less extensive compared with acute stage, and the ECV of chronic myocardial infarction is significantly elevated than normal but lower than acute conditions. In recent studies, native T1 was also an important predictor of clinical outcomes in patients with CAD.^{10,14} Native T1 and ECV can also be applied in the assessment of non-ischemic cardiomyopathies. Native T1 was mildly elevated in patients with hypertrophic cardiomyopathy and was highest in segments that subsequently

demonstrated LGE.¹⁶⁾ Native T1 was able to accurately discriminate hypertrophic cardiomyopathy from hypertensive heart disease,¹⁷⁾ and was better in discriminating cardiomyopathies from the normal hearts.¹⁸⁾

The T2 mapping can accurately and reliably detect areas of myocardial edema, a hallmark of acute inflammation,⁸⁾¹⁹⁾ and has been shown to be useful in acute myocardial infarction,²⁰⁾ myocarditis,²¹⁾ stress cardiomyopathy,²¹⁾ and cardiac allograft rejection.²²⁾ For this, conventional T2-weighted short- τ inversion recovery (T2-STIR) has been most commonly used and helpful in differentiating acute infarction from chronic infarction.²³⁾ However, as it depends on regional differences in myocardial signal intensity, its interpretation is qualitative and subjective.²⁴⁾²⁵⁾ T2 mapping is more reproducible than T2-STIR,²⁶⁾ and it can overcome this limitation of classic T2-STIR.²⁷⁾²⁸⁾ T2 values can be directly quantified in vivo, as a surrogate for myocardial water content.²⁹⁾ Normal T2 values acquired with steady-state free precession MRI have been reported to be 52.18 \pm 3.4 ms at 1.5T and 45.1 ms at 3T.³⁰⁾³¹⁾ Studies have shown that T2 values are increased in the state of advanced heart failure, representing decompensation and decreases after treatment.²⁸⁾ In a recent study, T2 mapping was superior compared with T1 mapping and ECV for the assessment of the myocarditis in patients with recent-onset heart failure with reduced ejection fraction.²⁷⁾

Recently, a novel MRI sequence named CMR multitasking that enables simultaneous T1 mapping, T1/T2 mapping, and time-resolved T1 mapping and hence markedly reduces the total acquisition time has been introduced.³²⁾ CMR multitasking uses a continuous acquisition approach, which conceptualizes the physiological motions and other dynamic processes as multiple time dimensions, making efficient quantitative CMR imaging possible without the use of electrocardiogram gating and breath holds.

Late gadolinium enhancement

The LGE technique is one of the most established methods in characterization of the myocardium using CMR imaging so far.²⁾⁷⁾ LGE is a T1-weighted technique that can detect and quantify areas of myocardial injury and cardiac infiltration in various cardiac diseases, and it has become the gold standard method for detecting myocardial scars. LGE uses the pattern and velocity of distribution and accumulation of the gadolinium-chelate contrast agent within the extracellular compartment of the myocardium.

Because the LGE pattern follows the pathophysiological process of the underlying disease, it helps identify the etiology of heart failure. In ischemic heart disease, the injury starts in the subendocardium and progresses into the transmural myocardium as ischemia continues.³³⁾ Thus, the LGE pattern in patients with CAD starts as subendocardial and extends transmurally, whereas that in patients with dilated cardiomyopathy demonstrates a linear mid-wall pattern in the interventricular septum.³³⁾³⁴⁾

Importantly, the presence and extent of LGE are significant prognostic indicators associated with an increased risk of future cardiac events, regardless of the underlying etiology or pattern of fibrosis.³⁵⁻³⁷⁾ Further, LGE can assess viability of the myocardium in ischemic and non-ischemic cardiac disease; thereby, it has the potential to guide the clinical decision.³⁷⁻⁴⁰⁾ The main limitation of LGE is that it is a marker of irreversible replacement fibrosis, the final pathophysiologic process of all cardiac diseases, and therefore is limited in assessing the early changes of cardiac diseases.⁴¹⁾⁴²⁾ Further, LGE is mostly useful in cardiac diseases which results in regional differences within the myocardium.³⁷⁾

Assessment of myocardial fiber orientation

CMR imaging can characterize the property of the myocardium and directly visualize the myocardial fiber architecture using diffusion tensor imaging (DTI).⁴³⁾⁴⁴⁾ Previous preclinical studies have demonstrated the ability of DTI to evaluate therapeutic responses of the myocardial microstructure, including stem cell or surgical treatment, in animal and human models.⁴⁵⁻⁴⁹⁾ Recently, technical advances have made the *in vivo* acquisition of DTI using clinical MR scanners possible in large animals and humans.⁵⁰⁻⁵²⁾ The DTI technique has been evaluated most frequently in hypertrophic cardiomyopathy and myocardial infarction.⁴⁵⁾⁵³⁾ Novel DTI was also feasible using a 3T clinical scanner.⁵⁴⁾

The clinical application of DTI has been limited because the ability of DTI to delineate the microstructure of the myocardium has been histologically validated only using destructive 2D methods that perturb the original myocardial fiber orientation.⁵⁵⁾⁵⁶⁾ The reliability of DTI was recently validated in normal and ischemic heart failure mice models, and the myocardial fiber orientation calculated by DTI was directly compared with histology using a non-destructive 3D method with the tissue-clearing technique.⁵⁷⁾ The correlations were significant in the normal and diseased models, showing the capability and accuracy of DTI for mapping the myocardial microstructure.⁵⁸⁾ Based on these observations, the clinical application of DTI using the clinical MRI system for characterizing the myocardial fiber architecture seems possible, and it can provide additional information to conventional viability characterizations (**Figure 1**).

Assessment of metabolic activity of the myocardium

To maintain its continuous contraction, the heart has a high rate of adenosine triphosphate (ATP) production and utilization.⁵⁹⁾ Previous studies have shown that cardiac dysfunction is associated with decreased myocardial ATP.⁶⁰⁾⁶¹⁾ Therefore, characterization of cardiac metabolism can be potentially useful in assessing disease progression and understanding the pathophysiology,⁵⁹⁾ and the direct measurement of metabolites involved in ATP synthesis can be used to assess myocardial ischemia, oxygenation, remodeling, and viability.⁶²⁾

The chemical exchange saturation transfer (CEST) technique has been developed to quantify metabolites and macromolecules.⁶³⁻⁶⁵⁾ In a recent study, CEST was able to map the creatine distribution within the myocardium to evaluate the metabolic activity in an animal model,⁶⁶⁾ and an optimized *in vivo* cardiac CEST sequence that maps free creatine in myocardial tissue, with a markedly reduced scan time by 10-fold and improved motion registration and signal

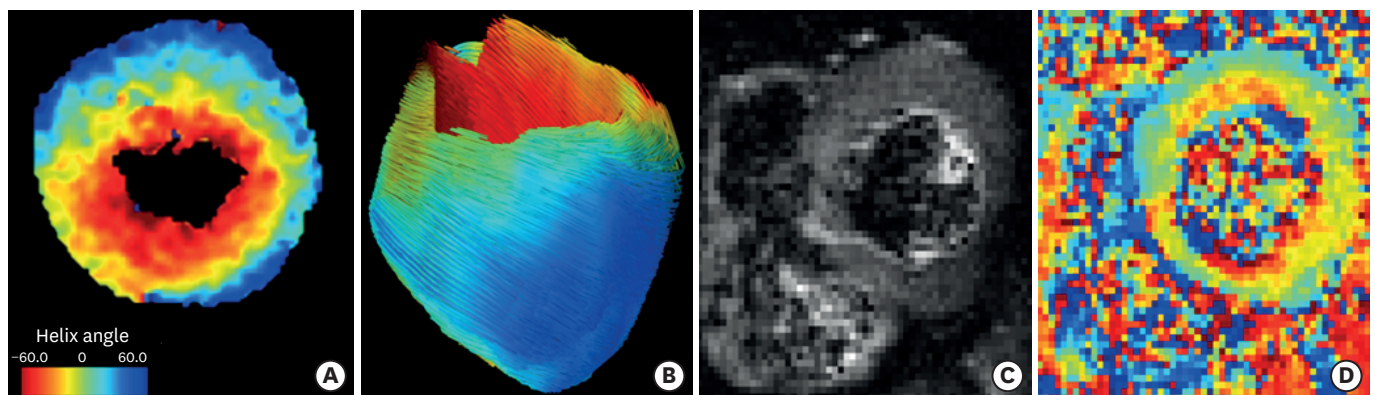


Figure 1. Representative image of diffusion tensor imaging (A) short-axis view of helix angle map and (B) tractography of the heart of a healthy mice, (C) diffusion image (left) and (D) corresponding helix angle map (right) of a patient with hypertrophic cardiomyopathy.

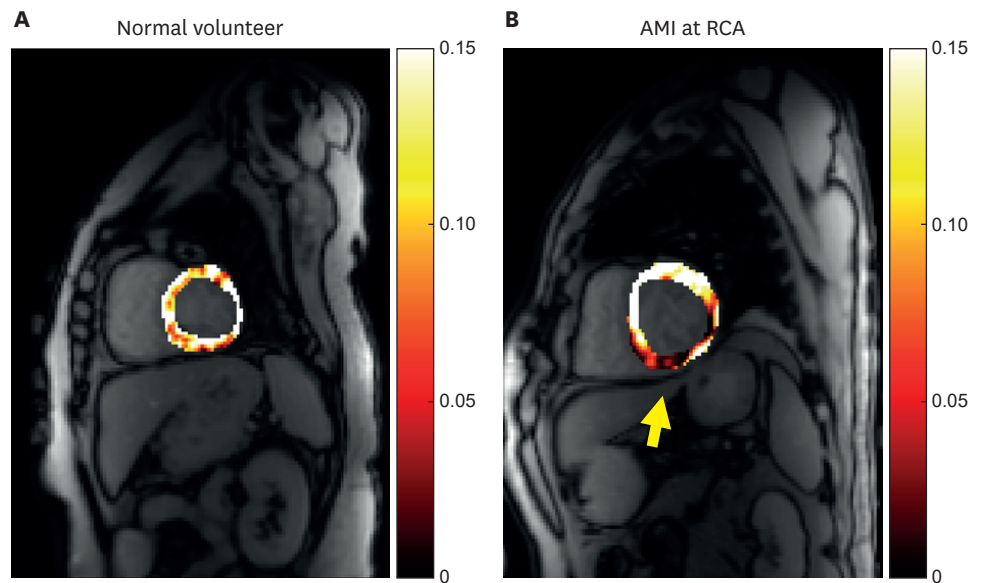


Figure 2. Representative images of chemical exchange saturation transfer in (A) a normal volunteer and (B) a patient with a history of acute myocardial infarction at right coronary artery. Arrow indicates the hypointensive segment corresponding to the inferior segment affected by acute myocardial infarction. AMI = acute myocardial infarction; RCA = right coronary artery.

calculation, has been developed.⁶⁷⁾ The feasibility of the sequence has been tested against LGE imaging as a reference in a porcine myocardial infarction model, and the sequence has been applied in a patient with chronic myocardial infarction. The creatine CEST signal was significantly reduced in the infarct region compared to remote myocardium in animal and human models, and it was well correlated with LGE (**Figure 2**).

ASSESSMENT OF MYOCARDIAL PERFORMANCE WITH FEATURE TRACKING

Quantification of the myocardial contractility using myocardial strain has been one of the major interests in cardiac imaging and mainly driven by speckle-tracking echocardiography, but CMR can also be used for the assessment of myocardial strain. Previous myocardial tagging-based CMR strain measurements were proven to be accurate for measuring regional myocardial strain, but required the acquisition of additional images and significant post-processing and hence limited its use in routine clinical practice.⁶⁸⁾ Recently, CMR feature tracking (FT) technique has enabled simultaneous assessment of both the left ventricular ejection fraction and strain using standard clinical steady-state free precession cine images.⁶⁹⁾⁷⁰⁾ In a meta-analysis of the normal reference ranges reported for global strain metrics measured by CMR-FT, a significant heterogeneity in strain measurements between studies were found which was not explained by either technical or physiological factors.⁶⁹⁾ To reduce this variability between vendors and to facilitate the development of vendor-independent normal references for the wider application of MR based strain measurements, the CMR-FT community is making a multivendor effort to standardize methodology for acquisition, post-processing, and reporting of CMR-FT strain results.⁶⁸⁾

CORONARY ARTERY PLAQUE IMAGING

Coronary magnetic resonance angiography

The modality of choice for assessing the coronary arteries remains invasive coronary angiography, which mainly focuses on delineating the vessel walls and luminal stenosis. As the needs for noninvasive imaging modalities that can evaluate coronary artery disease (CAD) emerge, attempts have been made to apply computed tomography (CT) and CMR imaging to the assessment of CAD. However, the application of CMR imaging in coronary artery imaging has been challenging because of the small size of coronary vessels and their complex motion; therefore, CMR imaging has lagged compared to CT angiography. Nevertheless, CMR imaging has several merits over CT, including superior soft-tissue contrast that possibly allows superior characterization of high-risk plaques and the lack of radiation exposure, which makes CMR imaging an excellent imaging modality for longitudinal studies. Further, as there is no calcium blooming effect with CMR imaging, it is possible to perform luminal assessment in patients with severe calcification. These advantages coupled with the development of fully digital systems, multichannel receiver coils, parallel imaging, and higher field strengths have improved the image quality of CMR imaging and made coronary magnetic resonance angiography (MRA) an attractive imaging modality for assessing CAD.⁷¹

Rapid sequences are essential in coronary MRA. For contrast-enhanced MRA, the spoiled gradient echo-like fast low-angle shot (e.g., TurboFLASH) is most commonly used.⁷¹ MRA can be also acquired without contrast using balanced steady-state free precession sequences, but gradient echo imaging with contrast is preferred in 3T or 7T MRI. The most commonly used contrast agent in coronary MRA is a chelated gadolinium-based agent. Contrast agents enhance the coronary lumen by shortening the T1 relaxation times of the blood pool. However, as gadolinium contrast is associated with nephrogenic systemic fibrosis, non-contrast MRA is gaining an important clinical role.⁷² The accuracy of coronary MRA in diagnosing luminal stenosis and quantitatively measuring the plaque burden has been validated in many previous studies.⁷³⁻⁷⁷ In meta-analyses, coronary MRA demonstrated an overall diagnostic accuracy of 72–79%, with an overall sensitivity of 87–89% and specificity of 70–72% when compared to invasive coronary angiography.^{74/76}

Quantitative assessment of coronary vessel wall thickness

Coronary MRA also enables the quantitative measurement of plaque thickness and plaque burden. Current technological development in coronary MRA has mainly focused on shortening the scan time, improving motion correction, and reducing the flow dependency. The conventional 2-dimensional (2D) black-blood vessel wall imaging sequence has been improved, and flow-independent black-blood methods are available along with 3-dimensional (3D) black-blood vessel wall MRA.⁷⁸⁻⁸⁰ Currently, the standard method used in coronary MRA is 2D measurements of plaque wall thickness.⁸¹ The feasibility of coronary MRA in the quantitative assessment of coronary arterial wall thickness has been validated against that of intravascular ultrasonography,^{82/83} and the increased plaque thickness detected by coronary MRA in asymptomatic patients was associated with subclinical coronary atherosclerosis.⁸⁴

Intraplaque hemorrhage by magnetic resonance imaging

Both histological and imaging studies have identified so-called “high-risk plaque features,” including positive remodeling, a thin fibrous cap, intraplaque hemorrhage, microcalcification, and a large necrotic core.⁸⁵⁻⁸⁷ CMR imaging can also be used to identify these plaque characteristics.

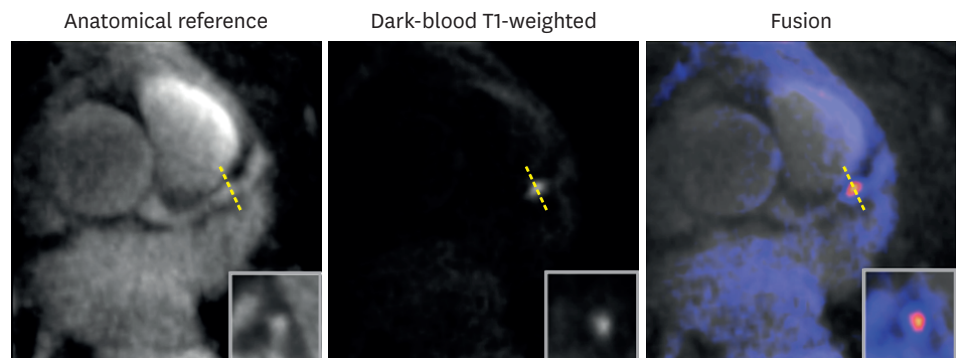


Figure 3. Representative image of pre-contrast coronary atherosclerosis T1-weighted characterization with integrated anatomical reference in a patient with a coronary hyperintense plaque in the mid left anterior descending artery.

Intraplaque hemorrhage has a high signal and very short T1 relaxation time because of methemoglobin, a main component of an acute thrombus. Therefore, detecting a freshly formed thrombus due to coronary plaque rupture or erosion using black-blood T1-weighted MRI as the method of choice is possible. In a prospective single-center study, high-intensity plaque, defined as plaque with a plaque-to-myocardial signal intensity ratio (PMR) >1.4, was associated with an increased risk of subsequent adverse coronary events in patients with stable CAD.⁸⁸⁾ The increased PMR was also an independent predictor for adverse clinical outcomes at follow-up. The high-intensity signal of these plaques significantly reduced after intensive statin treatment,⁸⁹⁾ demonstrating the feasibility of evaluating the therapeutic response using coronary T1-weighted MRI.

One of the main limitations of these coronary T1-weighted MRI sequences based on conventional Cartesian acquisition and navigator gating is the intolerably long acquisition time. Because prior coronary T1-weighted MRI techniques heavily attenuate the signals from surrounding structures, the anatomic reference (coronary MRA) needs to be acquired separately and co-registered with T1-weighted images afterward in order to localize the high-intensity signal of the coronary vasculature. Furthermore, the coverage has been limited to proximal segments, as spatial resolution was often anisotropic.⁸⁸⁾

In this regard, we developed a highly accelerated magnetic resonance (MR) technique named coronary atherosclerosis T1-weighted characterization with integrated anatomical reference (CATCH) using a motion-compensated interleaved acquisition scheme that provides coronary T1-weighted images and integrated anatomical reference in one acquisition time, thereby shortening the total scan time to less than 25 minutes.⁹⁰⁾ This technique has been validated against optical coherence tomography, and coronary high-intensity plaques detected by CATCH were associated with lipid profiles and high-risk plaque characteristics detected by invasive coronary imaging (Figure 3).⁹⁰⁾

NONINVASIVE MEASUREMENT OF THE PRESSURE GRADIENT

Fractional flow reserve (FFR) is defined as the ratio of the blood pressure distal to a site of stenosis (P_d) and the aortic pressure (P_a) during maximal hyperemia, and it represents the functional significance of coronary stenosis.⁹¹⁾ Because the measurement of FFR requires

drug-induced hyperemia, instantaneous wave-free ratio (iFR), a drug-free method, which measures P_a and P_d during the middle to end diastolic phase, has been introduced.⁹²⁾ Previous studies have shown that $FFR \leq 0.80$ and $iFR \leq 0.89$ accurately identify significant stenoses that cause myocardial ischemia and require revascularization better than diameter stenoses.⁹³⁾⁹⁴⁾

Using the Navier-Stokes analysis, an FFR-like index using phase-contrast MRI called MR-iFR has been developed.⁹⁵⁾ In a preliminary study, the feasibility of the noninvasive blood pressure gradient and velocity measurement using phase-contrast MRI was demonstrated in phantoms and patients undergoing invasive FFR.⁹⁵⁾ MR-iFR showed good overall reproducibility of coronary flow velocity and excellent correlation with invasive measurements.

CURRENT LIMITATIONS OF CARDIAC MAGNETIC RESONANCE

Currently, CMR is not as widely used as like cardiac CT, mainly because of the long acquisition time and limitations in spatial and temporal resolution. To overcome these limitations, new techniques including compressed sensing and parallel imaging are being applied in various sequences.⁹⁶⁾ One of the major obstacles for the clinical application of CMR is also the lack of standardized protocol and the variation in CMR values related to equipment and sequences. Although efforts have been made including the publication of guidelines for the standardized protocol, image interpretation and post processing,²⁾³⁾ the interchangeability between different vendors and magnet strengths are limited. The reference ranges for “normal” values for each CMR sequence are needed to be established as the difference between manufacturers, magnetic field strengths, and sequences varies widely. Further, the full clinical utility of various CMR values are yet unknown because only limited cardiac diseases have been studied for each sequence in separate conditions. Multi-center, multivendor clinical trials are needed to fully establish the clinical utility of CMR in various cardiac diseases.

SUMMARY

CMR imaging offers comprehensive images of the heart in patients with various cardiac diseases. The prognostic value of CMR imaging is well established, and emerging novel technologies demonstrate the potential of CMR imaging to even change the clinical decision-making process. Along with the rapid technological development, CMR imaging is able to provide new insights into understanding the pathophysiologic process of underlying cardiac disease, and it can help physicians choose the best treatment strategies. Although several limitations, including the high cost and time-consuming process, have limited the widespread clinical use of CMR imaging so far, recent advances in software and hardware technologies have made the future more promising.

REFERENCES

1. Stuber M, Botnar RM, Fischer SE, et al. Preliminary report on in vivo coronary MRA at 3 Tesla in humans. *Magn Reson Med* 2002;48:425-9.

[PUBMED](#) | [CROSSREF](#)

2. Kramer CM, Barkhausen J, Flamm SD, Kim RJ, Nagel E; Society for Cardiovascular Magnetic Resonance Board of Trustees Task Force on Standardized Protocols. Standardized cardiovascular magnetic resonance (CMR) protocols 2013 update. *J Cardiovasc Magn Reson* 2013;15:91.
[PUBMED](#) | [CROSSREF](#)
3. Schulz-Menger J, Bluemke DA, Bremerich J, et al. Standardized image interpretation and post processing in cardiovascular magnetic resonance: Society for Cardiovascular Magnetic Resonance (SCMR) board of trustees task force on standardized post processing. *J Cardiovasc Magn Reson* 2013;15:35.
[PUBMED](#) | [CROSSREF](#)
4. Plein S, Ryf S, Schwitter J, Radjenovic A, Boesiger P, Kozerke S. Dynamic contrast-enhanced myocardial perfusion MRI accelerated with k-t sense. *Magn Reson Med* 2007;58:777-85.
[PUBMED](#) | [CROSSREF](#)
5. Cheng AS, Pegg TJ, Karamitsos TD, et al. Cardiovascular magnetic resonance perfusion imaging at 3-tesla for the detection of coronary artery disease: a comparison with 1.5-tesla. *J Am Coll Cardiol* 2007;49:2440-9.
[PUBMED](#) | [CROSSREF](#)
6. Patel AR, Kramer CM. Role of cardiac magnetic resonance in the diagnosis and prognosis of nonischemic cardiomyopathy. *JACC Cardiovasc Imaging* 2017;10:1180-93.
[PUBMED](#) | [CROSSREF](#)
7. Hundley WG, Bluemke DA, Finn JP, et al. ACCF/ACR/AHA/NASCI/SCMR 2010 expert consensus document on cardiovascular magnetic resonance: a report of the American College of Cardiology Foundation Task Force on Expert Consensus Documents. *J Am Coll Cardiol* 2010;55:2614-62.
[PUBMED](#) | [CROSSREF](#)
8. Messroghli DR, Moon JC, Ferreira VM, et al. Clinical recommendations for cardiovascular magnetic resonance mapping of T1, T2, T2* and extracellular volume: A consensus statement by the Society for Cardiovascular Magnetic Resonance (SCMR) endorsed by the European Association for Cardiovascular Imaging (EACVI). *J Cardiovasc Magn Reson* 2017;19:75.
[PUBMED](#) | [CROSSREF](#)
9. Ugander M, Oki AJ, Hsu LY, et al. Extracellular volume imaging by magnetic resonance imaging provides insights into overt and sub-clinical myocardial pathology. *Eur Heart J* 2012;33:1268-78.
[PUBMED](#) | [CROSSREF](#)
10. Puntmann VO, Carr-White G, Jabbour A, et al. Native T1 and ECV of noninfarcted myocardium and outcome in patients with coronary artery disease. *J Am Coll Cardiol* 2018;71:766-78.
[PUBMED](#) | [CROSSREF](#)
11. Kawel N, Nacif M, Zavodni A, et al. T1 mapping of the myocardium: intra-individual assessment of the effect of field strength, cardiac cycle and variation by myocardial region. *J Cardiovasc Magn Reson* 2012;14:27.
[PUBMED](#) | [CROSSREF](#)
12. Haaf P, Garg P, Messroghli DR, Broadbent DA, Greenwood JP, Plein S. Cardiac T1 mapping and extracellular volume (ECV) in clinical practice: a comprehensive review. *J Cardiovasc Magn Reson* 2016;18:89.
[PUBMED](#) | [CROSSREF](#)
13. Mavrogeni S, Apostolou D, Argyriou P, et al. T1 and T2 mapping in cardiology: "mapping the obscure object of desire". *Cardiology* 2017;138:207-17.
[PUBMED](#) | [CROSSREF](#)
14. Kammerlander AA, Marzluf BA, Zotter-Tufaro C, et al. T1 mapping by CMR imaging: from histological validation to clinical implication. *JACC Cardiovasc Imaging* 2016;9:14-23.
[PUBMED](#) | [CROSSREF](#)
15. Sado DM, Flett AS, Banyersad SM, et al. Cardiovascular magnetic resonance measurement of myocardial extracellular volume in health and disease. *Heart* 2012;98:1436-41.
[PUBMED](#) | [CROSSREF](#)
16. Dass S, Suttie JJ, Piechnik SK, et al. Myocardial tissue characterization using magnetic resonance noncontrast T1 mapping in hypertrophic and dilated cardiomyopathy. *Circ Cardiovasc Imaging* 2012;5:726-33.
[PUBMED](#) | [CROSSREF](#)
17. Hinojar R, Varma N, Child N, et al. T1 mapping in discrimination of hypertrophic phenotypes: hypertensive heart disease and hypertrophic cardiomyopathy: findings from the international T1 multicenter cardiovascular magnetic resonance study. *Circ Cardiovasc Imaging* 2015;8:8.
[PUBMED](#) | [CROSSREF](#)
18. Puntmann VO, Voigt T, Chen Z, et al. Native T1 mapping in differentiation of normal myocardium from diffuse disease in hypertrophic and dilated cardiomyopathy. *JACC Cardiovasc Imaging* 2013;6:475-84.
[PUBMED](#) | [CROSSREF](#)
19. Dweck MR, Puntman V, Vesey AT, Fayad ZA, Nagel E. MR imaging of coronary arteries and plaques. *JACC Cardiovasc Imaging* 2016;9:306-16.
[PUBMED](#) | [CROSSREF](#)

20. Verhaert D, Thavendiranathan P, Giri S, et al. Direct T2 quantification of myocardial edema in acute ischemic injury. *JACC Cardiovasc Imaging* 2011;4:269-78.
[PUBMED](#) | [CROSSREF](#)
21. Thavendiranathan P, Walls M, Giri S, et al. Improved detection of myocardial involvement in acute inflammatory cardiomyopathies using T2 mapping. *Circ Cardiovasc Imaging* 2012;5:102-10.
[PUBMED](#) | [CROSSREF](#)
22. Usman AA, Taimen K, Wasielewski M, et al. Cardiac magnetic resonance T2 mapping in the monitoring and follow-up of acute cardiac transplant rejection: a pilot study. *Circ Cardiovasc Imaging* 2012;5:782-90.
[PUBMED](#) | [CROSSREF](#)
23. Friedrich MG, Abdel-Aty H, Taylor A, Schulz-Menger J, Messroghli D, Dietz R. The salvaged area at risk in reperfused acute myocardial infarction as visualized by cardiovascular magnetic resonance. *J Am Coll Cardiol* 2008;51:1581-7.
[PUBMED](#) | [CROSSREF](#)
24. McAlindon E, Pufulete M, Lawton C, Angelini GD, Bucciarelli-Ducci C. Quantification of infarct size and myocardium at risk: evaluation of different techniques and its implications. *Eur Heart J Cardiovasc Imaging* 2015;16:738-46.
[PUBMED](#) | [CROSSREF](#)
25. Jeserich M, Föll D, Olschewski M, et al. Evidence of myocardial edema in patients with nonischemic dilated cardiomyopathy. *Clin Cardiol* 2012;35:371-6.
[PUBMED](#) | [CROSSREF](#)
26. McAlindon EJ, Pufulete M, Harris JM, et al. Measurement of myocardium at risk with cardiovascular MR: comparison of techniques for edema imaging. *Radiology* 2015;275:61-70.
[PUBMED](#) | [CROSSREF](#)
27. Bohnen S, Radunski UK, Lund GK, et al. Performance of T1 and T2 mapping cardiovascular magnetic resonance to detect active myocarditis in patients with recent-onset heart failure. *Circ Cardiovasc Imaging* 2015;8:8.
[PUBMED](#) | [CROSSREF](#)
28. Verbrugge FH, Bertrand PB, Willems E, et al. Global myocardial oedema in advanced decompensated heart failure. *Eur Heart J Cardiovasc Imaging* 2017;18:787-94.
[PUBMED](#) | [CROSSREF](#)
29. Friedrich MG. Myocardial edema--a new clinical entity? *Nat Rev Cardiol* 2010;7:292-6.
[PUBMED](#) | [CROSSREF](#)
30. Giri S, Shah S, Xue H, et al. Myocardial T2 mapping with respiratory navigator and automatic nonrigid motion correction. *Magn Reson Med* 2012;68:1570-8.
[PUBMED](#) | [CROSSREF](#)
31. von Knobelsdorff-Brenkenhoff F, Prothmann M, Dieringer MA, et al. Myocardial T1 and T2 mapping at 3 T: reference values, influencing factors and implications. *J Cardiovasc Magn Reson* 2013;15:53.
[PUBMED](#) | [CROSSREF](#)
32. Christodoulou AG, Shaw JL, Nguyen C, et al. Magnetic resonance multitasking for motion-resolved quantitative cardiovascular imaging. *Nat Biomed Eng* 2018;2:215-26.
[PUBMED](#) | [CROSSREF](#)
33. Dweck MR, Williams MC, Moss AJ, Newby DE, Fayad ZA. Computed tomography and cardiac magnetic resonance in ischemic heart disease. *J Am Coll Cardiol* 2016;68:2201-16.
[PUBMED](#) | [CROSSREF](#)
34. McCrohon JA, Moon JC, Prasad SK, et al. Differentiation of heart failure related to dilated cardiomyopathy and coronary artery disease using gadolinium-enhanced cardiovascular magnetic resonance. *Circulation* 2003;108:54-9.
[PUBMED](#) | [CROSSREF](#)
35. Kwong RY, Chan AK, Brown KA, et al. Impact of unrecognized myocardial scar detected by cardiac magnetic resonance imaging on event-free survival in patients presenting with signs or symptoms of coronary artery disease. *Circulation* 2006;113:2733-43.
[PUBMED](#) | [CROSSREF](#)
36. Schelbert EB, Cao JJ, Sigurdsson S, et al. Prevalence and prognosis of unrecognized myocardial infarction determined by cardiac magnetic resonance in older adults. *JAMA* 2012;308:890-6.
[PUBMED](#) | [CROSSREF](#)
37. Kim RJ, Wu E, Rafael A, et al. The use of contrast-enhanced magnetic resonance imaging to identify reversible myocardial dysfunction. *N Engl J Med* 2000;343:1445-53.
[PUBMED](#) | [CROSSREF](#)

38. Gutberlet M, Fröhlich M, Mehl S, et al. Myocardial viability assessment in patients with highly impaired left ventricular function: comparison of delayed enhancement, dobutamine stress MRI, end-diastolic wall thickness, and TI201-SPECT with functional recovery after revascularization. *Eur Radiol* 2005;15:872-80.
[PUBMED](#) | [CROSSREF](#)
39. Leong DP, Chakrabarty A, Shipp N, et al. Effects of myocardial fibrosis and ventricular dyssynchrony on response to therapy in new-presentation idiopathic dilated cardiomyopathy: insights from cardiovascular magnetic resonance and echocardiography. *Eur Heart J* 2012;33:640-8.
[PUBMED](#) | [CROSSREF](#)
40. Bodí V, Sanchis J, López-Lereu MP, et al. Usefulness of a comprehensive cardiovascular magnetic resonance imaging assessment for predicting recovery of left ventricular wall motion in the setting of myocardial stunning. *J Am Coll Cardiol* 2005;46:1747-52.
[PUBMED](#) | [CROSSREF](#)
41. Iles LM, Ellims AH, Llewellyn H, et al. Histological validation of cardiac magnetic resonance analysis of regional and diffuse interstitial myocardial fibrosis. *Eur Heart J Cardiovasc Imaging* 2015;16:14-22.
[PUBMED](#) | [CROSSREF](#)
42. Kim RJ, Fieno DS, Parrish TB, et al. Relationship of MRI delayed contrast enhancement to irreversible injury, infarct age, and contractile function. *Circulation* 1999;100:1992-2002.
[PUBMED](#) | [CROSSREF](#)
43. Garrido L, Wedeen VJ, Kwong KK, Spencer UM, Kantor HL. Anisotropy of water diffusion in the myocardium of the rat. *Circ Res* 1994;74:789-93.
[PUBMED](#) | [CROSSREF](#)
44. Mekkaoui C, Reese TG, Jackowski MP, Bhat H, Sosnovik DE. Diffusion MRI in the heart. *NMR Biomed* 2017;30:30.
[PUBMED](#) | [CROSSREF](#)
45. Sosnovik DE, Mekkaoui C, Huang S, et al. Microstructural impact of ischemia and bone marrow-derived cell therapy revealed with diffusion tensor magnetic resonance imaging tractography of the heart in vivo. *Circulation* 2014;129:1731-41.
[PUBMED](#) | [CROSSREF](#)
46. Walker JC, Guccione JM, Jiang Y, et al. Helical myofiber orientation after myocardial infarction and left ventricular surgical restoration in sheep. *J Thorac Cardiovasc Surg* 2005;129:382-90.
[PUBMED](#) | [CROSSREF](#)
47. Chen Y, Ye L, Zhong J, et al. The structural basis of functional improvement in response to human umbilical cord blood stem cell transplantation in hearts with postinfarct LV remodeling. *Cell Transplant* 2015;24:971-83.
[PUBMED](#) | [CROSSREF](#)
48. Lombardi R, Rodriguez G, Chen SN, et al. Resolution of established cardiac hypertrophy and fibrosis and prevention of systolic dysfunction in a transgenic rabbit model of human cardiomyopathy through thiol-sensitive mechanisms. *Circulation* 2009;119:1398-407.
[PUBMED](#) | [CROSSREF](#)
49. Nguyen CT, Dawkins J, Bi X, Marbán E, Li D. Diffusion tensor cardiac magnetic resonance reveals exosomes from cardiosphere-derived cells preserve myocardial fiber architecture after myocardial infarction. *JACC Basic Transl Sci* 2018;3:97-109.
[PUBMED](#) | [CROSSREF](#)
50. Nielles-Vallespin S, Mekkaoui C, Gatehouse P, et al. In vivo diffusion tensor MRI of the human heart: reproducibility of breath-hold and navigator-based approaches. *Magn Reson Med* 2013;70:454-65.
[PUBMED](#) | [CROSSREF](#)
51. Nguyen C, Fan Z, Sharif B, et al. In vivo three-dimensional high resolution cardiac diffusion-weighted MRI: a motion compensated diffusion-prepared balanced steady-state free precession approach. *Magn Reson Med* 2014;72:1257-67.
[PUBMED](#) | [CROSSREF](#)
52. Aliotta E, Wu HH, Ennis DB. Convex optimized diffusion encoding (CODE) gradient waveforms for minimum echo time and bulk motion-compensated diffusion-weighted MRI. *Magn Reson Med* 2017;77:717-29.
[PUBMED](#) | [CROSSREF](#)
53. Nguyen C, Lu M, Fan Z, et al. Contrast-free detection of myocardial fibrosis in hypertrophic cardiomyopathy patients with diffusion-weighted cardiovascular magnetic resonance. *J Cardiovasc Magn Reson* 2015;17:107.
[PUBMED](#) | [CROSSREF](#)
54. Nguyen C, Fan Z, Xie Y, et al. In vivo diffusion-tensor MRI of the human heart on a 3 tesla clinical scanner: An optimized second order (M2) motion compensated diffusion-preparation approach. *Magn Reson Med* 2016;76:1354-63.
[PUBMED](#) | [CROSSREF](#)

55. Gilbert SH, Benoist D, Benson AP, et al. Visualization and quantification of whole rat heart laminar structure using high-spatial resolution contrast-enhanced MRI. *Am J Physiol Heart Circ Physiol* 2012;302:H287-98.
[PUBMED](#) | [CROSSREF](#)
56. Hales PW, Schneider JE, Burton RA, Wright BJ, Bollensdorff C, Kohl P. Histo-anatomical structure of the living isolated rat heart in two contraction states assessed by diffusion tensor MRI. *Prog Biophys Mol Biol* 2012;110:319-30.
[PUBMED](#) | [CROSSREF](#)
57. Chung K, Wallace J, Kim SY, et al. Structural and molecular interrogation of intact biological systems. *Nature* 2013;497:332-7.
[PUBMED](#) | [CROSSREF](#)
58. Lee SE, Nguyen C, Yoon J, et al. Three-dimensional cardiomyocytes structure revealed by diffusion tensor imaging and its validation using a tissue-clearing technique. *Sci Rep* 2018;8:6640.
[PUBMED](#) | [CROSSREF](#)
59. Doenst T, Nguyen TD, Abel ED. Cardiac metabolism in heart failure: implications beyond ATP production. *Circ Res* 2013;113:709-24.
[PUBMED](#) | [CROSSREF](#)
60. Reibel DK, Rovetto MJ. Myocardial ATP synthesis and mechanical function following oxygen deficiency. *Am J Physiol* 1978;234:H620-4.
[PUBMED](#)
61. Garlid KD, Dos Santos P, Xie ZJ, Costa AD, Paucek P. Mitochondrial potassium transport: the role of the mitochondrial ATP-sensitive K(+) channel in cardiac function and cardioprotection. *Biochim Biophys Acta* 2003;1606:1-21.
[PUBMED](#) | [CROSSREF](#)
62. Dzeja PP, Redfield MM, Burnett JC, Terzic A. Failing energetics in failing hearts. *Curr Cardiol Rep* 2000;2:212-7.
[PUBMED](#) | [CROSSREF](#)
63. Zhou J, Payen JF, Wilson DA, Traystman RJ, van Zijl PC. Using the amide proton signals of intracellular proteins and peptides to detect pH effects in MRI. *Nat Med* 2003;9:1085-90.
[PUBMED](#) | [CROSSREF](#)
64. Gilad AA, McMahon MT, Walczak P, et al. Artificial reporter gene providing MRI contrast based on proton exchange. *Nat Biotechnol* 2007;25:217-9.
[PUBMED](#) | [CROSSREF](#)
65. Cai K, Haris M, Singh A, et al. Magnetic resonance imaging of glutamate. *Nat Med* 2012;18:302-6.
[PUBMED](#) | [CROSSREF](#)
66. Haris M, Singh A, Cai K, et al. A technique for in vivo mapping of myocardial creatine kinase metabolism. *Nat Med* 2014;20:209-14.
[PUBMED](#) | [CROSSREF](#)
67. Zhou Z, Nguyen C, Chen Y, et al. Optimized CEST cardiovascular magnetic resonance for assessment of metabolic activity in the heart. *J Cardiovasc Magn Reson* 2017;19:95.
[PUBMED](#) | [CROSSREF](#)
68. Salerno M. Feature tracking by CMR: a “double feature”? *JACC Cardiovasc Imaging* 2018;11:206-8.
[PUBMED](#) | [CROSSREF](#)
69. Vo HQ, Marwick TH, Negishi K. MRI-derived myocardial strain measures in normal subjects. *JACC Cardiovasc Imaging* 2018;11:196-205.
[PUBMED](#) | [CROSSREF](#)
70. Ogawa R, Kido T, Nakamura M, et al. Diagnostic capability of feature-tracking cardiovascular magnetic resonance to detect infarcted segments: a comparison with tagged magnetic resonance and wall thickening analysis. *Clin Radiol* 2017;72:828-34.
[PUBMED](#) | [CROSSREF](#)
71. Regenfus M, Ropers D, Achenbach S, et al. Noninvasive detection of coronary artery stenosis using contrast-enhanced three-dimensional breath-hold magnetic resonance coronary angiography. *J Am Coll Cardiol* 2000;36:44-50.
[PUBMED](#) | [CROSSREF](#)
72. Grobner T, Prischl FC. Gadolinium and nephrogenic systemic fibrosis. *Kidney Int* 2007;72:260-4.
[PUBMED](#) | [CROSSREF](#)
73. Kim WY, Danias PG, Stuber M, et al. Coronary magnetic resonance angiography for the detection of coronary stenoses. *N Engl J Med* 2001;345:1863-9.
[PUBMED](#) | [CROSSREF](#)

74. Schuetz GM, Zacharopoulou NM, Schlattmann P, Dewey M. Meta-analysis: noninvasive coronary angiography using computed tomography versus magnetic resonance imaging. *Ann Intern Med* 2010;152:167-77.
[PUBMED](#) | [CROSSREF](#)
75. Jahnke C, Paetsch I, Nehrke K, et al. Rapid and complete coronary arterial tree visualization with magnetic resonance imaging: feasibility and diagnostic performance. *Eur Heart J* 2005;26:2313-9.
[PUBMED](#) | [CROSSREF](#)
76. Di Leo G, Fisci E, Secchi F, et al. Diagnostic accuracy of magnetic resonance angiography for detection of coronary artery disease: a systematic review and meta-analysis. *Eur Radiol* 2016;26:3706-18.
[PUBMED](#) | [CROSSREF](#)
77. Yonezawa M, Nagata M, Kitagawa K, et al. Quantitative analysis of 1.5-T whole-heart coronary MR angiograms obtained with 32-channel cardiac coils: a comparison with conventional quantitative coronary angiography. *Radiology* 2014;271:356-64.
[PUBMED](#) | [CROSSREF](#)
78. Andia ME, Henningsson M, Hussain T, et al. Flow-independent 3D whole-heart vessel wall imaging using an interleaved T2-preparation acquisition. *Magn Reson Med* 2013;69:150-7.
[PUBMED](#) | [CROSSREF](#)
79. Fayad ZA, Fuster V, Fallon JT, et al. Noninvasive in vivo human coronary artery lumen and wall imaging using black-blood magnetic resonance imaging. *Circulation* 2000;102:506-10.
[PUBMED](#) | [CROSSREF](#)
80. Xie G, Bi X, Liu J, et al. Three-dimensional coronary dark-blood interleaved with gray-blood (cDIG) magnetic resonance imaging at 3 tesla. *Magn Reson Med* 2016;75:997-1007.
[PUBMED](#) | [CROSSREF](#)
81. Desai MY, Lai S, Barmet C, Weiss RG, Stuber M. Reproducibility of 3D free-breathing magnetic resonance coronary vessel wall imaging. *Eur Heart J* 2005;26:2320-4.
[PUBMED](#) | [CROSSREF](#)
82. Gerretsen S, Kessels AG, Nelemans PJ, et al. Detection of coronary plaques using MR coronary vessel wall imaging: validation of findings with intravascular ultrasound. *Eur Radiol* 2013;23:115-24.
[PUBMED](#) | [CROSSREF](#)
83. He Y, Zhang Z, Dai Q, et al. Accuracy of MRI to identify the coronary artery plaque: a comparative study with intravascular ultrasound. *J Magn Reson Imaging* 2012;35:72-8.
[PUBMED](#) | [CROSSREF](#)
84. Miao C, Chen S, Macedo R, et al. Positive remodeling of the coronary arteries detected by magnetic resonance imaging in an asymptomatic population: MESA (Multi-Ethnic Study of Atherosclerosis). *J Am Coll Cardiol* 2009;53:1708-15.
[PUBMED](#) | [CROSSREF](#)
85. Puchner SB, Liu T, Mayrhofer T, et al. High-risk plaque detected on coronary CT angiography predicts acute coronary syndromes independent of significant stenosis in acute chest pain: results from the ROMICAT-II trial. *J Am Coll Cardiol* 2014;64:684-92.
[PUBMED](#) | [CROSSREF](#)
86. Naghavi M, Libby P, Falk E, et al. From vulnerable plaque to vulnerable patient: a call for new definitions and risk assessment strategies: part I. *Circulation* 2003;108:1664-72.
[PUBMED](#) | [CROSSREF](#)
87. Kolodgie FD, Gold HK, Burke AP, et al. Intraplaque hemorrhage and progression of coronary atheroma. *N Engl J Med* 2003;349:2316-25.
[PUBMED](#) | [CROSSREF](#)
88. Noguchi T, Kawasaki T, Tanaka A, et al. High-intensity signals in coronary plaques on noncontrast T1-weighted magnetic resonance imaging as a novel determinant of coronary events. *J Am Coll Cardiol* 2014;63:989-99.
[PUBMED](#) | [CROSSREF](#)
89. Noguchi T, Tanaka A, Kawasaki T, et al. Effect of intensive statin therapy on coronary high-intensity plaques detected by noncontrast T1-weighted imaging: the AQUAMARINE pilot study. *J Am Coll Cardiol* 2015;66:245-56.
[PUBMED](#) | [CROSSREF](#)
90. Xie Y, Kim YJ, Pang J, et al. Coronary atherosclerosis T1-weighted characterization with integrated anatomical reference: comparison with high-risk plaque features detected by invasive coronary imaging. *JACC Cardiovasc Imaging* 2017;10:637-48.
[PUBMED](#) | [CROSSREF](#)
91. Pijls NH, Van Gelder B, Van der Voort P, et al. Fractional flow reserve. A useful index to evaluate the influence of an epicardial coronary stenosis on myocardial blood flow. *Circulation* 1995;92:3183-93.
[PUBMED](#) | [CROSSREF](#)

92. Sen S, Escaned J, Malik IS, et al. Development and validation of a new adenosine-independent index of stenosis severity from coronary wave-intensity analysis: results of the ADVISE (ADenosine Vasodilator Independent Stenosis Evaluation) study. *J Am Coll Cardiol* 2012;59:1392-402.
[PUBMED](#) | [CROSSREF](#)
93. Escaned J, Echavarría-Pinto M, Garcia-Garcia HM, et al. Prospective assessment of the diagnostic accuracy of instantaneous wave-free ratio to assess coronary stenosis relevance: results of ADVISE II International, Multicenter Study (ADenosine Vasodilator Independent Stenosis Evaluation II). *JACC Cardiovasc Interv* 2015;8:824-33.
[PUBMED](#) | [CROSSREF](#)
94. Tonino PA, De Bruyne B, Pijls NH, et al. Fractional flow reserve versus angiography for guiding percutaneous coronary intervention. *N Engl J Med* 2009;360:213-24.
[PUBMED](#) | [CROSSREF](#)
95. Deng Z, Fan Z, Lee SE, et al. Noninvasive measurement of pressure gradient across a coronary stenosis using phase contrast (PC)-MRI: a feasibility study. *Magn Reson Med* 2017;77:529-37.
[PUBMED](#) | [CROSSREF](#)
96. Saloner D, Liu J, Haraldsson H. MR physics in practice: how to optimize acquisition quality and time for cardiac MR imaging. *Magn Reson Imaging Clin N Am* 2015;23:1-6.
[PUBMED](#) | [CROSSREF](#)